

ANNEXE

GUICHAINVILLE / LE VIEIL-ÉVREUX - LONG-BUISSON : LUMINESCENCE DATING REPORT

Jean-Luc SCHWENNINGER

1: Comments on the interpretation of the results

Introduction

The samples were collected by J.-L. Schwenninger assisted by D. Cliquet and J.- P. Lautridou on the 3rd of June 2003 from two machine excavated trenches at Guichainville / Le Vieil-Évreux - Long-Buisson (North: 49°00'; East: 1°11'). Samples X1650 and X1651 were both collected from trench T.29 (see Figure 109). The former was obtained from a yellow silt deposit located at a depth of 76cm from the top of the excavated trench and overlying a thin layer of small stones ('cailloutis'). The latter was obtained further down in the same section at a depth of 225 cm and underlying a yellowish brown silty unit considered to be a palaeosol. Samples X1652 and X1653 are two duplicate samples collected from a light grey silt unit located towards the base of trench T.31 at a depth of 192cm from the top of the section (see Figure 110). This silt was very dry and compact and difficult to sample.

Optically stimulated luminescence (OSL) age estimates reported in this report are based on small amounts of sand-sized quartz grains (90-125µm), extracted from each sample and mounted on aluminium discs as multigrain single aliquots (see section 4).

All measurements were made using a modified single aliquot regenerative dose measurement protocol further outlined in section 4.1 and according to measurement procedures described in section 4.2. Results are summarized in Table 25 and further details regarding individual samples may be found in Appendix 1. Dose rates were calculated from in-situ NaI gamma-ray spectrometer measurements. Supplementary instrumental neutron activation analysis (INAA) was carried out in order to assess the beta dose rates and to provide an independent check of radioisotope concentration in the sediments (see Table 26).

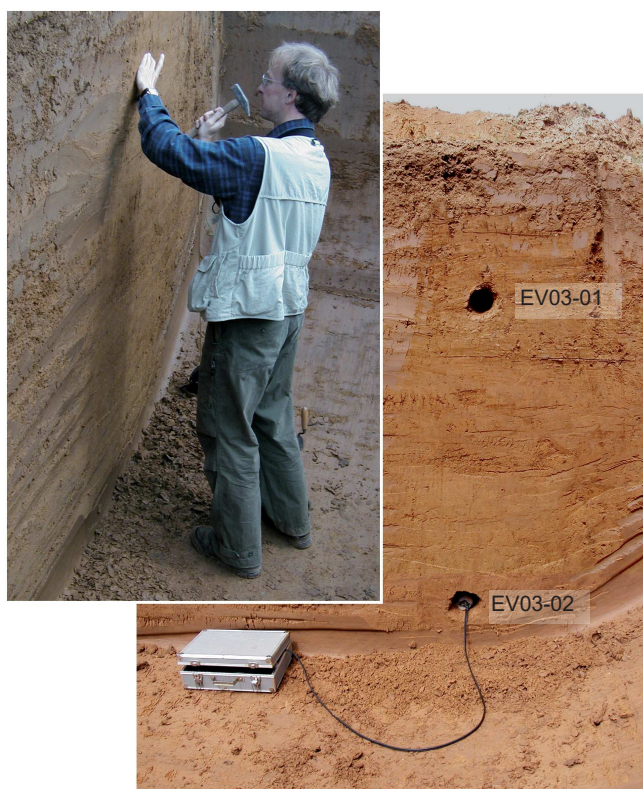


Figure 109 - Position of samples for OSL dating in trench T.29 (photos Dominique Cliquet, MCC).

Figure 109 - Localisation des échantillons prélevés pour OSL dans la tranchée T. 29 (clichés Dominique Cliquet).

Results

For all the samples measured from this site, no infrared stimulated luminescence (IRSL) values above normal background levels were observed in any of the aliquots, suggesting good

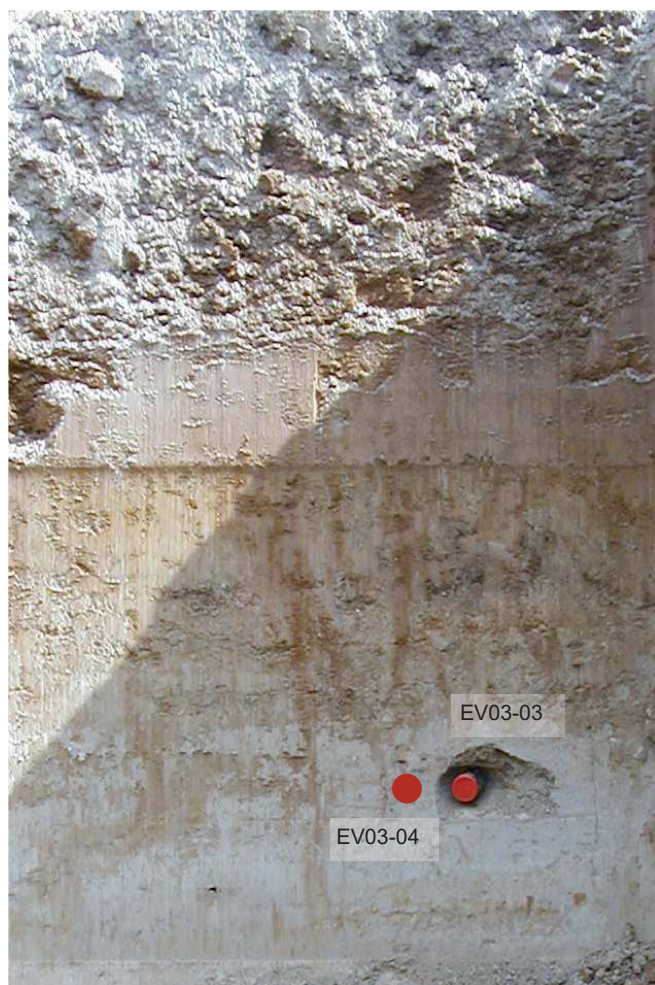


Figure 110 - Position of samples for OSL dating in trench T.31 (photo Dominique Cliquet, MCC).

Figure 110 - Localisation des échantillons prélevés pour OSL dans la tranchée T. 31 (cliché Dominique Cliquet).

quartz separation had been achieved with no problems relating to potential signal interference from feldspar contaminants.

Sample X1650: All aliquots were characterized by very low thermal transfer (average 1.20%) with good recycling ratios (average 0.98). Measurements on six aliquots produced a well constrained series of palaeodose estimates ranging from 83 to 93Gy with a weighted mean value of 89.53 ± 6 Gy. As expected from windblown sediments of this nature, there is no evidence to suggest signs of partial bleaching and all the mineral grains are likely to have been fully reset at deposition. The sample produced a final age estimate of 39.2ka with a small error of 4.7% at the one sigma confidence level.

Sample X1651: As noted for the previous sample, excellent recycling (average 1.00) and very low thermal transfer (<2%) values were measured. However, the majority of aliquots were close to saturation and the distribution of palaeodose values suggest a significant degree of scatter. Four aliquots were close to saturation and in this instance, only a minimum palaeodose estimate of circa 340Gy could be calculated. Two non saturated aliquots produced estimates of 315Gy and 265Gy, corresponding to respective age estimates of 127ka and 107ka. This sample may have been affected by partial bleaching or post depositional mixing of grains and consequently, the data may only be considered as providing, a safe minimum age estimate with an optical date considered to be in excess of 100ka. A mean weighted palaeodose of 299.15 ± 25.33 is obtained from the two non-saturated palaeodose estimates. This would suggest a date of 120.2 ± 11.7 ka and a depositional age roughly corresponding to oxygen isotope stage 5. **The limited number of aliquots however, implies that this age estimate may not be considered to be reliable and the results must be interpreted with caution.**

Field code	Location	Lab. code	Depth (m)	Palaeodose (Gy)	Dose rate (mGy/a)	Age (ka)
EV03-01	Trench T29	X1650	0,96	$89,53 \pm 1,60$	$2,28 \pm 0,09$	$39,21 \pm 1,87$
EV03-02	Trench T29	X1651	2,45	> 300 Gy ($299,15 \pm 25,33$)	$2,49 \pm 0,11$	> 120 ($120,2 \pm 11,7$)
EV03-03	Trench T31	X1652	2,42	> 450 Gy	$2,37 \pm 0,09$	> 200
EV03-04	Trench T31	X1653	2,42	> 450 Gy	$2,41 \pm 0,10$	> 200

Table 25 - Summary of optically stimulated luminescence (OSL) dating results. Sand-sized (90-125 μ m) quartz grain were measured using a modified multigrain single aliquot regenerative dose (SAR) measurement procedure (Murray and Wintle 2000, Banerjee *et al.* 2001) in order to calculate the palaeodose. Gamma dose rates were measured in-situ using a portable γ -ray spectrometer. The beta dose rate was derived from the concentrations of U, Th and K determined by instrumental neutron activation analysis (INAA) as shown in Table 27. The cosmic-ray contribution to the total dose rate was derived from published data by Prescott and Hutton (1994) taking into account the height of the overburden, altitude and geographical position of the site.

Tableau 25 - Résumé des résultats des datations par stimulation lumineuse optique (OSL)

Field code	Location	Lab. code	Moisture	Potassium (%)	Thorium (%)	Uranium (%)
EV03-01	Trench T29	X1650	18,9	1,13	12,2	1,46
EV03-02	Trench T29	X1651	18,1	1,38	12,1	2,2
EV03-03	Trench T31	X1652	16	0,98	13,2	2,94
EV03-04	Trench T31	X1653	15,5	1,04	12,8	2,97

Table 26 - Moisture content and results of instrumental neutron activation analysis (INAA) used for dose rate calculations.

Tableau 26 - Teneur en humidité et les résultats de l'analyse par activation neutronique instrumentale (INAA) utilisés pour le calcul du débit de dose calculs.

Samples X1652 and X1653: These are two duplicate samples collected from the same sedimentary context (see Figure 111) and hence should provide similar age estimates. Both are characterized by very good mean recycling ratios and low thermal transfer but the luminescence measurements revealed that all aliquots were saturated. **A likely age in excess of 200ka may be inferred** from the mean saturation point (~500Gy) on the dose response curve.

Conclusion

The OSL dating results from Guichainville / Le Vieil-Évreux - Long-Buisson provide a basic chronological framework for this site. The results provide clear evidence that the widespread deposits of loess encountered across Normandy can provide sufficient coarse grained pure quartz material for optical dating without having to rely on traditional polymineral fine grain preparations which can lead to erroneous age determinations. The main limitation of these windblown silt deposits with respect to luminescence dating, is their relatively high dose rate (circa 2.3Gy/ka) which leads to early saturation of the luminescence signal and appears to restrict dating applications to sediments younger than circa 150ka.

2: The physical basis of luminescence dating

When ionising radiation (predominantly alpha, beta, or gamma radiation) interacts with an insulating crystal lattice (such as quartz or feldspar), a net redistribution of electronic charge takes place. Electrons are stripped from the outer shells of atoms and though most return immediately, a proportion escape and become trapped at meta-stable sites within the lattice. This charge redistribution continues for the duration of the radiation exposure and the amount of trapped charge is therefore related to both the duration and the intensity of radiation exposure. Even though trapped at meta-stable sites, electrons become 'free' if the crystal is subjected to heat or exposed to light. Once liberated, a free electron may become trapped once again or may return to a vacant position caused by the absence of a previously displaced electron (a 'hole'). This latter occurrence is termed 'recombination' and the location of the hole is described as the 'recombination centre'. As recombination occurs, a proportion of the energy of the electron is dissipated. Depending upon the nature of the centre where recombination occurs, this energy is expelled as heat and/or light. Therefore, when the crystal grain is either heated or illuminated following natural or artificial laboratory irradiation (the 'dose') the total amount of light emitted (luminescence) is directly related to the number of liberated electrons and available recombination sites. This is the fundamental principle upon which luminescence dating is based.

In cases where the duration of dosing is not known (as is the case for dating), estimates can be made from laboratory measurements. The response (the sensitivity) of the sample to radiation dose (ie the amount of light observed for a given amount of laboratory radiation, usually β -radiation) must be established. From this relationship the equivalent radiation exposure required to produce the same amount of light as that observed following the natural environmental dose can be determined, and

is termed the palaeodose or 'equivalent dose' (De). The palaeodose (measured in Gy) is therefore an estimate of the total dose absorbed during the irradiation period. When the dose rate (the amount of radiation per unit time, measured in $\mu\text{Gy/a}$) is measured or calculated from measured concentrations of radionuclides, the duration of the dosing period can be calculated using the equation:

$$\text{Duration of dosing period} = \text{Palaeodose} / \text{dose rate.}$$

The technique of optical dating was first applied to quartz by Huntley *et al.* (1985), and methodological details were further developed by Smith *et al.* (1986) and Rhodes (1988). The technique was demonstrated to work well for aeolian samples by Smith *et al.* (1990), and has further proved to provide useful age estimates for a range of sedimentary contexts ranging from aeolian (eg Stokes *et al.* 1997) to glacial contexts (Owen *et al.* 1997). Further developmental research has introduced palaeodose measurement protocols that use a 'single aliquot regenerative dose' (SAR) protocol (Murray and Wintle 2000). These protocols generally have the potential to provide improved accuracy (e.g. through correction of sensitivity change, interpolation rather than extrapolation of palaeodose values) as well as increased precision. In some cases they may also provide an indication of incomplete zeroing of the luminescence signal at the time of deposition. Recent research within the laboratory (Rhodes *et al.* 2003) has demonstrated the high precision and accuracy that may be achieved with this technique.

3: Sample preparation

The laboratory procedures were designed to yield pure quartz, of a particular grain size range, from the natural sediment samples. In order to obtain this material, samples were taken through a standard preparation procedure, as outlined below. All laboratory treatments were performed under low intensity laboratory safe-lighting, from purpose-built filtered sodium lamps (emitting at 588 nm).

After removal of the exposed ends of the sampling containers, the unexposed central portion of the sample was wet-sieved and the 90-125 μm grain size was used for dating (see Appendix 1 for details of specific samples). The chosen fraction was treated with hydrochloric acid (HCl) to remove carbonate and then treated in concentrated HF (48%) for 100 minutes. This treatment serves two purposes: (i) to dissolve feldspar grains, and (ii) to remove (etch) the outer surface of quartz grains (the only part of each quartz grain exposed during burial to natural alpha radiation). Any heavy minerals present were subsequently removed by gravity separation using a sodium polytungstate solution at 2.68 g.cm⁻³. Finally, each sample was re-sieved to remove heavily etched grains. The order of the heavy liquid separation and second sieving are on occasion reversed for practical reasons, and for samples with extremely low yields, either or both of these treatments may be omitted after careful consideration. The prepared quartz samples were mounted on 1 cm diameter aluminium discs for luminescence measurement using viscous silicone oil.

Various tests for sample purity are made. Sub-samples of the prepared material are examined using optical microscopy and

the sample is exposed (within the RisØ measurement system) to infrared (IR) light. Quartz generally does not produce measurable IR luminescence at room temperature whereas feldspar, which can suffer from anomalous fading of the infrared stimulated luminescence (IRSL) and OSL signals, or may be less rapidly bleached in some environments, produces an intense luminescence when stimulated with IR. The presence of a strong IRSL signal is therefore used as an indication for the presence of feldspar contaminants and is a criterion for rejection. In the rare cases where samples are rejected due to presence of high levels of IRSL, the prepared sediment sample is treated for ~ 2 weeks in concentrated H_2SiF_6 (silica-saturated HF) which effectively dissolves non-quartz material. If following this treatment, IRSL persists then the sample is subjected to a further two week H_2SiF_6 acid treatment before proceeding to the dating phase (luminescence measurement) and the results are interpreted with caution and the possible contamination of the sample discussed.

The measurement sequence adopted for dating all the samples included a post-IR blue OSL procedure (Banerjee *et al.* 2001) designed to deplete any feldspar contribution to the OSL signal, by preceding each OSL measurement with an IRSL measurement. The IR exposure reduces the size of feldspar contributions, besides providing an alternative means to determine a palaeodose. For samples with strong IRSL signals, significant feldspar contribution to the OSL may remain, and this is considered in the interpretation of the dates.

In order to determine the attenuating effect of pore water on the environmental dose rate of the sediments, additional samples were collected in the field and hermetically sealed. The moisture content of the sample was determined in the laboratory by weighing the sample before and after oven drying at 50°.

4: Measurement procedures

The single aliquot regenerative-dose (SAR) protocol

The SAR method is a regeneration procedure where the light level of the natural signal is converted into Gy via an interpolation between regenerated (ie known dose) points. The natural and regenerated signals are measured using the same aliquot. Sensitivity change commonly observed in quartz TL/OSL has previously precluded meaningful results being obtained this way. A key development reported by Murray and Wintle (2000) is that sample (aliquot) sensitivity is monitored following each OSL measurement (L_i) using the OSL response to a common test dose (S_i). Plots of L_i / S_i provide the necessary (sensitivity change corrected) data for interpolation. The procedure is further outlined in Figure 111.

Steps 1-6 are repeated n times in order to produce the data points required for interpolation (the first dose β_1 being zero, to give a measure of the natural signal). Typically $n=7$ (ie the natural plus 6 regeneration points, including one zero dose point and one repeat point). PH1 and PH2 are usually different although Murray and Wintle (2000) report no dependence of the palaeodose on either (over the range of 200-280°C). The OSL

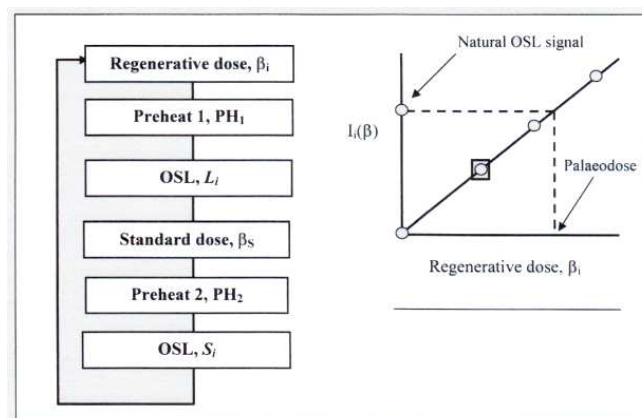


Figure 111 - The SAR method. The procedure illustrated here is described in further detail in the text.

Figure 111 - La méthode SAR. La procédure illustrée ici est décrite plus en détail dans le texte.

signal is integrated over the initial part of the decay (to ~10% of initial intensity) and the background is taken as the light level measured at the end of each OSL measurement.

Murray and Wintle (2000) have introduced two further steps in to the measurement procedure. The first is the re-measurement of the first regenerated data point (indicated by the box in the explanatory Figure 110 above). The ratio of the two points (the “recycling ratio”) provides an assessment of the efficacy of the sensitivity correction and the accuracy of the technique (large differences being suggestive of an ineffective technique). The recycling ratio (ideally unity) is typically in the range 0.95-1.05. The second additional step is a measurement of the regenerated OSL due to zero dose. This value gives a measure of the degree of thermal transfer to the trap(s) responsible for OSL during pre-heating. The ratio of this value to the natural OSL value (both corrected for sensitivity change) gives the “thermal transfer ratio” and ideally this should be in the range of 0.005-0.020.

Measurement procedures and conditions

Luminescence measurements were made using automated RisØ luminescence measurement equipment. There are currently three different systems within our Luminescence Dating Laboratory that can be used for routine dating, the major difference between them being the optical stimulation sources. In two systems, optical excitation is provided by filtered blue diodes (emitting ~410-510nm), and in the third a filtered Halogen lamp (emitting ~420-560nm) is used. In all three systems, infrared stimulation is also provided using either an array of IR diodes or a single IR laser diode (depending on the measurement system). Luminescence is detected in the UV region on all systems, using EMI 9635Q bialkali photomultiplier tubes, filtered with Hoya U340 glass filters. Sample irradiation is provided in all cases by sealed ^{90}Sr sources at a rate of 1.5-3 Gy/minute depending on the system used.

The mean palaeodose for each sample was obtained from 6 aliquots (see Appendix 3 for further details regarding the statistics used in palaeodose and error calculations). All OSL measurements were made at 125°C (to ensure no re-trapping of charge to the 110°C TL trap during measurement) for between 50 and

100s, depending on the measurement system used. The signal detected in the initial 1st to 2nd seconds (with the stable background count rate from the last 12 to 24 seconds subtracted) was corrected for sensitivity using the OSL signal regenerated by a subsequent beta dose (135). To ensure removal of unstable OSL components, removal of dose quenching effects, and to stimulate re-trapping and ensure meaningful comparison between naturally and laboratory irradiated signals, pre-heating was performed prior to each OSL measurement. Following each regenerative dose (β_i) and the natural dose, a pre-heat (PH1) at 260°C for 10s was used. After each test dose (135) a pre-heat (PH2) of 220°C for 10s was applied (see 'The single aliquot regenerative-dose (SAR) protocol' for further details of the SAR method). All the OSL measurements incorporated a post-IR blue OSL stage in which each OSL measurement is preceded by an IRSL measurement at 50°C, to reduce the effects of any residual feldspar grains (Banerjee *et al*

2001) but the SAR procedure is otherwise unchanged.

For every sample, a routine internal laboratory procedure referred to as DELIA (De Luminescence Initial Assessment) was applied prior to the main SAR measurement in order to determine their approximate palaeodose value. This consisted in the use of a simplified version of the SAR measurement protocol applied to a limited number of three test discs in order to determine the internal variability, the OSL and TL signal form and sensitivity, as well as the magnitude of any IRSL signals. This considerably assists in the optimal selection of regenerative and test dose values, number of aliquots to measure, and the pre-heat combination selected. Quartz samples showing high levels of IRSL at this stage are given an extended (usually 14 days) treatment in fluorosilicic acid (H_2SiF_6). None of the samples from Guichainville / Le Vieil-Évreux - Long-Buisson required additional H_2SiF_6 treatment.

Appendix 1 : Details of radioactivity data and age calculations

Sample number	EV03-01	EV03-02	EV03-03	EV03-04
Laboratory code	X1650	X1651	X1652	X1653
Comments		Close to saturation	Saturated	Saturated
Palaeodose (Gy)	89,53	-299,15	> 450,00	> 450,00
Uncertainty	2,401	26,027	41,000	41,000
Error measured	1,6	25,33	40,00	40,00
Additional systematic calibration error 2%	1,791	5,983	9,000	9,000
Grain size				
Min. grain size (μm)	90	90	90	90
Max. grain size (μm)	125	125	125	125
External gamma-dose (Gy/ka)	1,067	1,072	1,054	1,054
Error	0,003	0,003	0,002	0,002
Measured concentrations				
standard fractional error	0,050	0,050	0,050	0,050
% K	1,130	1,380	0,983	1,040
error (%K)	0,057	0,069	0,049	0,052
Th (ppm)	12,200	12,100	13,200	12,800
error (ppm)	0,610	0,605	0,660	0,640
U (ppm)	1,460	2,200	2,940	2,970
error (ppm)	0,073	0,110	0,147	0,149
Cosmic dose calculations				
Depth (m)	0,960	2,450	2,420	2,420
error (m)	0,100	0,100	0,100	0,100
Average overburden density ($\text{g.cm}^{\wedge}3$)	1,900	1,900	1,900	1,900
error ($\text{g.cm}^{\wedge}3$)	0,100	0,100	0,100	0,100
Latitude (deg.), north positive	49,000	49,000	49,000	49,000
Longitude (deg.), east positive	1,000	1,000	1,000	1,000
Altitude (m above sea-level)	125,000	125,000	125,000	125,000
Cosmic dose rate ($\mu\text{Gy/ka}$)	0,189	0,156	0,157	0,157
error	0,024	0,013	0,013	0,013
Moisture content				
Moisture (water / wet sediment)	0,189	0,181	0,160	0,155
error	0,050	0,050	0,050	0,050
Total dose rate, Gy/ka	2,28	2,49	2,37	2,41
error	0,09	0,11	0,09	0,10
% error	3,94	4,30	3,93	4,02
AGE (ka)	39,21	(120,21)	> 200	> 200
error	1,87	11,67		
% error	4,77	9,71		

Sample number	EV03-01	EV03-02	EV03-03	EV03-04
Laboratory code	X1650	X1651	X1652	X1653
Average beta-attenuation				
standard fractional error	0,050	0,050	0,050	0,050
Natural U	0,900	0,900	0,900	0,900
error	0,045	0,045	0,045	0,045
Th- 232	0,852	0,852	0,852	0,852
error	0,043	0,043	0,043	0,043
K-40	0,962	0,962	0,962	0,962
error	0,048	0,048	0,048	0,048
Dose rate conversion (Gy/ka)				
standard fractional error	0,050	0,050	0,050	0,050
U (ppm)				
Beta	0,146	0,146	0,146	0,146
error	0,007	0,007	0,007	0,007
Gamma	0,000	0,000	0,000	0,000
error	0,000	0,000	0,000	0,000
Th (ppm)				
Beta	0,027	0,027	0,027	0,027
error	0,001	0,001	0,001	0,001
Gamma	0,000	0,000	0,000	0,000
error	0,000	0,000	0,000	0,000
K (%)				
Beta	0,782	0,782	0,782	0,782
error	0,039	0,039	0,039	0,039
Gamma	0,000	0,000	0,000	0,000
error	0,000	0,000	0,000	0,000
Cosmic dose				
Geomagnetic latitude	51,7	51,7	51,7	51,7
Dc (Gy/ka), 55N G. lat, 0 km Alt.	0,185	0,153	0,153	0,153
error	0,023	0,013	0,013	0,013
Moisture				
F	0,482	0,470	0,436	0,428
error	0,090	0,092	0,097	0,098
W	0,482	0,470	0,436	0,428
error	0,090	0,092	0,097	0,098
WF	0,232	0,221	0,190	0,183
error	0,062	0,061	0,059	0,059
Age uncertainties	1,000	1,000	1,000	1,000
dDR/K	0,583	0,589	0,608	0,612
dDR/dC(B, K)	0,842	1,040	0,764	0,814
dDR/dA (K)	0,685	0,846	0,621	0,662
dDR/dTh	0,018	0,018	0,019	0,019
dDR/dC(B, Th)	8,051	8,074	9,086	8,869
dDR/dDa (Th)	0,258	0,259	0,291	0,284
dDR/dU	0,102	0,103	0,106	0,107
dDR/dC(B, U)	0,698	0,706	0,728	0,733
dDR/dA (U)	0,165	0,252	0,347	0,353
dDR/dW	-0,480	-0,580	-0,510	-0,521
dDR/dF	-0,480	-0,580	-0,510	-0,521
dDR/C(G, K)	0,893	1,102	0,808	0,860
dDR/C(G, Th)	9,644	9,665	10,852	10,588
dDR/dC(G, U)	1,154	1,757	2,417	2,457
dDR/dCosmic	1,000	1,000	1,000	1,000
dage/dDe	0,438	0,402	0,422	0,415
Dage/dDr	-17,180	-48,310	-80,190	-77,660

Appendix 2 : Dose rate determination

Radiation dose is measured in energy units of Gray (Gy), the standard SI unit of absorbed dose (1 Gy = 1 Joule/kg). The measurement of dose rate (or annual dose) can be made using a variety of different methods. For most samples, the majority of the environmental dose rate is due to the radioactive decay of unstable isotopes of potassium (K), uranium (U) and daughter isotopes, and thorium (Th) and daughter isotopes. A further small fraction comes from the cosmic dose rate, and is a function of altitude, geomagnetic latitude, and overburden thickness and density (Prescott and Hutton 1994). Water content attenuates the environmental dose rate, and uncertainties in the average of this value over the burial period may often form a significant contribution to the overall uncertainty in the age estimate.

In-situ gamma-ray spectrometry

Portable gamma spectrometer readings may be taken at each sampling location. The probe (housing a NaI scintillator crystal) is inserted into a deepened hole excavated following the retrieval of the OSL sample. Measurements typically take up to one hour and result in the direct estimation of the total in-situ gamma radiation field. The spectra are also used to estimate contributions from U, Th, and K individually. Through comparison to known concentration standards, quantitative estimates of U, Th, and K concentrations are made.

Instrumental Neutron Activation Analysis

A representative sub-sample (typically 10-20g, though as little as 80mg may be used with specialised procedures) of the sample is sent for commercial analysis. The analysis involves an initial (neutron) irradiation of each sample. This causes the creation of many new short-lived isotopes whose concentration depend on the bulk chemical composition of the original sample. This leaves the samples in a highly unstable (ie radioactive) state. The different gamma emissions from the radioactive decay of the sample are then measured using high resolution gamma- spectrometry. These measurements yield estimates of U, Th, and K concentration. The measurement of K and Th are usually precise, though samples with low levels of U may be below the detection limit for this element, depending on the interferences from other isotopes. The direct measurement of a small volume renders this method very well suited for the estimation of beta dose rate.

Moisture content of the sample

Moisture within the pore spaces of sediments absorbs α , β and γ -radiation. As a result, less is absorbed by the mineral grains. It is therefore important to assess the present day water content of the sediment and to make some assessment of the variability of moisture throughout the burial period of the sample. The moisture correction factors outlined in Aitken (1985) and taken from Zimmermann (1971) are used in the age calculation (Appendix 1).

Cosmic dose rate

The contribution of cosmic radiation to the total dose rate

is calculated as a function of (geomagnetic) latitude, altitude, burial depth, and average over-burden density, according to the formulae of Prescott and Hutton (1994).

Radiation attenuation factors

For coarse grains, the portion of the sample that receives an α -dose is removed by HF etching. Therefore, no consideration of the α -dose is made during the age calculation. β -particles (electrons) are significantly attenuated (ie a large fraction of the energy is absorbed) as the β -particle passes through a grain. Account of this effect is needed in order to correctly estimate the dose received by the 'average' grain. The so-called 'attenuation factors' are taken from the empirical work of Mejdahl (1979).

The γ -dose is assumed to be unaffected by attenuation as the penetration of gamma-rays through sediments is several orders of magnitude greater than ($\sim 10^5$ times) the size of individual grains. Consequently, no attenuation factors are applied to the γ -dose.

Results for the U, Th (ppm), and K (%) concentration of each sample, together with the other parameters used in the age calculation, are provided in Appendix 1.

Appendix 3 : Statistics and error calculation

The calculated age depends on the estimate of total absorbed dose (D_e) and the dose rate (DR). Both of these estimates have uncertainties associated with them. This appendix gives general details of how the 'error' (the statistical uncertainty) is calculated for each term and combined with the errors on other terms to give an overall estimate of uncertainty on the OSL age estimate.

Palaeodose estimation

As described in a previous section, individual estimates of palaeodose also referred to as D_e are obtained from each of the aliquots (sub-samples) measured, using the SAR technique. The value of the D_e is obtained by interpolating between the points of the dose response curve. Statistical uncertainties are calculated for each of the individual points and also on the interpolated value of D_e . Typically, 12 aliquots are measured for each sample.

Each of the points on the growth curve is defined as:

$$I(\beta)_i = \frac{L_i - f.l_i}{S_i - f.s_i} \quad \text{Equation 1}$$

where L_i is the integrated (initial) OSL from the regeneration dose and l_i is the measured background signal, S_i is the integrated (initial) OSL from the test dose (see Section 2) and s_i is the background; f is a scaling factor included to take account of the difference in duration of the L_i , S_i and l_i , s_i measurements.

The error on each dose-response data point (see Figure 110) is calculated by propagating 'counting statistics' errors (assuming Poisson statistics) from the integration of raw OSL data. The error on each term in Equation 1 is given by the square-root of the value. For example, the range for L_i is given by $L_i \pm \sqrt{L_i}$,

The errors on each value are propagated in the standard way (see below) to give the uncertainty of $I(\beta)$.

In cases where the dose response can be (locally) approximated by a straight line, a weighted least squares linear fit is used. The errors in this case are calculated analytically using standard formulae.

In cases where the dose response is significantly non-linear, a single saturating exponential function is used to describe the dose response (a Simplex algorithm is used for fitting in this case). Occasionally an extra linear term is added to the exponential term in order to better describe the form of the dose response, although this is not commonly necessary. The uncertainty for non-linear fitting is calculated using a Monte-Carlo method in which ‘random samples’ of the dose response data are taken (assuming normally distributed probabilities) and used to obtain the palaeodose value. The spread in these values is then used to calculate the error on the mean palaeodose for each aliquot, giving a range for each palaeodose of $D_{ei} \pm \sigma D_{ei}$.

Once the individual D_e values have been obtained from each aliquot (and the associated uncertainties calculated) the values are grouped to give a final overall estimate of D_e . The final D_e estimate is calculated using a weighted average. The weight of each D_e is referred to as W_i and defined as:

$$w_i = \frac{1}{\sigma D_{ei}^2} / \sum_i \frac{1}{\sigma D_{ei}^2} \quad \text{Equation 2}$$

The weighted mean is defined as:

$$\bar{D}_e = \sum_i D_{ei} \cdot w_i \quad \text{Equation 3}$$

The weighted standard error, $\sigma_{\bar{x}_w}$, is calculated from:

$$\sigma_{\bar{x}_w} = \sqrt{\frac{\sum_i w_i (D_{ei} - \bar{D}_e)^2}{1 - \frac{1}{n}}} / \sqrt{n} \quad \text{Equation 4}$$

Where n is the number of aliquots. The range of the weighted

mean D_e is then defined as:

$$\bar{D}_e \pm \sigma_{\bar{x}_w} \quad \text{Equation 5}$$

Slight modifications to the approach outlined above are made in special circumstances, though in most cases this description is sufficient.

Dose rate

The errors on the dose rate are due to errors in a range of values, for example, the concentration of U, Th, and K, as well as the water content of the sample. The individual components of the dose rate calculation are shown in Appendix 1. The uncertainty on the overall dose rate is calculated by combining the uncertainties according to the standard propagation formula given below.

Age calculation

The calculated age is obtained from dividing the mean palaeodose (Equation 3) by the total dose rate (Appendix 1). The uncertainty on the final age estimate is calculated using the error propagation formula given below. All calculations were performed using software developed within the laboratory.

Standard error propagation

If a calculated value (y) is calculated using a function (f) which contains terms $X_1, X_2, X_3, \dots, X_n$, then,

$$y = f(x_1, x_2, x_3, \dots, x_n) \quad \text{Equation 6}$$

Each term (X_i) has an associated uncertainty with a range expressed as $X_i \pm \sigma_{xi}$. The overall error of y can be calculated through the addition of the partial derivatives of y with respect to each term. Formally, this is written as:

$$\sigma_y = \sqrt{\sum_i \left(\frac{\partial y}{\partial x_i} \cdot \sigma_{xi} \right)^2} \quad \text{Equation 7}$$

giving a range for y as $y \pm \sigma_y$.